ELSEVIER

Catalysis Today 28 (1996) 59–69

CATALYSIS TODAY

Study of the structure of niobium oxide by X-ray absorption fine structure and surface science techniques

Takashi Ushikubo [a,*], Yasuo Koike [a], Keisuke Wada [b], Lei Xie [c], Dezheng Wang [c], Xiexian Guo [c]

[a] *Yokohama Research Center, Mitsubishi Chemical Corporation, 1000 Kamoshida-chou, Aoba-ku, Yokohama 227, Japan*

[b] *Research and Development Division, Mitsubishi Chemical Corporation, 2-5-2 Marunouchi, Chiyoda-ku, Tokyo 100, Japan*

[c] *State Key Laboratory of Catalysis, Dalian Institute of Chemical Physics, Chinese Academy of Sciences, P.O. Box 110, Dalian 116023, China*

Abstract

The structure of niobium oxides was investigated by using XAFS and surface science techniques. The origin of acidic property and catalysis of niobium oxide is discussed by these results. From the EXAFS analysis, the structure of highly acidic hydrated niobium oxide is different from those of T-Nb_2O_5 and $K_8Nb_6O_{19}$, which has been previously demonstrated as the structure of hydrated niobium oxide, because Nb–Nb and Nb–O distances are significantly different from each other. There are at least two types of Nb–O bonds, a tetrahedral form and an octahedral form are existing for hydrated niobium oxide. The excess of negative charge is present for Nb–O bond by applying Tanabe's hypothesis to single metal oxide consisting of at least two metal–O forms with different coordination number. That seems to be the origin of the acidity of hydrated niobium oxide. The ordered niobium oxides thin film on Pt(111) and their defect face were prepared by using UHV surface analysis apparatus. The oxygen vacancies of niobium oxide on Pt(111) were created by Ar^+ ion bombardment. H_2O and CH_3OH exhibit associated adsorption on the ordered NbO_x and Nb_2O_5 surface and dissociative adsorption on the defect Nb_2O_5 surface at room temperature. On the ordered NbO_x and Nb_2O_5 surface, no evidence of ethene adsorption at 200 K is found by HREELS, although ethene adsorbs molecularly on the defect Nb_2O_5 surface with a π-complex formation. These results imply that oxygen vacancies of NbO_x surface play an important role on the adsorption of the molecules.

Keywords: Niobium oxide; X-ray absorption fine structure; Surface science

1. Introduction

Niobium oxide has drawn attention as catalysts. Especially, amorphous hydrated niobium oxide is known to be an unusual solid acid that retains a high acid strength ($H_0 = -5.6$) on the surface even in the presence of water [1]. Several kinds of reactions catalyzed by the hydrated niobium oxide have been reported, e.g., the gas-phase hydration of ethene, the gas-phase esterification of acetic acid [2] and acrylic acid [3] and the liquid-phase hydration of succinonitrile [4]. Hydrated niobium oxide crystallizes at 853 K and the strong acid property of the hydrated niobium oxide disappears when it is heated at higher temperatures than 800 K.

* Corresponding author. Tel.: (+81-45) 9633188, fax: (+81-45) 9634254, e-mail: ushikubo@rc.m-kagaku.co.jp.

SSDI 0920-5861(95)00230-8

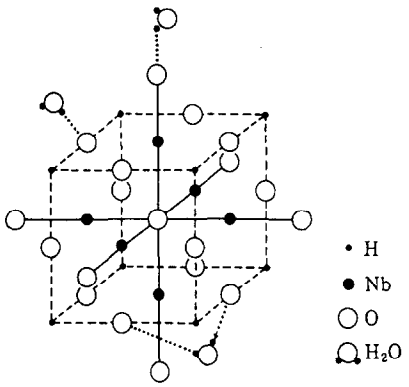

Fig. 1. Structure of niobium isopolyacid ($H_8Nb_6O_{19}$), which is the presumed structure model of hydrated niobium oxide.

There has been little knowledge about the structure of hydrated niobium oxide, because it is amorphous in an active form. Neumann [5] and Sen and coworkers [6] demonstrated that the structure of hydrated niobium oxide was an isopolyacid of composition $H_8Nb_6O_{19}$, as shown in Fig. 1. It could be depicted by the presence of the eight protons above eight triangular faces of the octahedron formed by six niobium atoms.

XAFS is one of the effective techniques for determining the structure of amorphous substance. So, we tried to study the structure of hydrated niobium oxide by using XAFS.

On the other hand, it has been known that the acid–base and adsorption properties of metal oxides are changed by the surface structure. So, the method of using an epitaxial oxide film on a transition metal single crystal as a model surface of the corresponding oxide was proposed [7] and used [7–9] to solve the difficulties in obtaining oxide single crystals, charging problems with insulator surfaces and bulk impurities in the oxide bulk that segregate to the surface upon heating. Previously, we reported the preparation of three types of thin films of niobium oxide on Pt(111); NbO_x, Nb_2O_5 and Ar^+-bombarded Nb_2O_5 [10]. The thin films were made up of a high density of small crystallites on an epitaxial monolayer. The structure similarity with supported two-dimensional Nb oxide monolayers with Nb=O surface sites of highly distorted NbO_6 octahedra was suggested by HREELS. Defect surface was produced by Ar^+ ion bombardment that selectively removed oxygen. This gives an oxygen deficient surface and was characterized by HREELS, LEED, UPS and ISS. The interaction of molecules with surface of metal oxides is important for understanding of the catalysis by the metal oxides. In this study, we wish to report the adsorption of water, methanol and ethene on the ordered and defect Nb_2O_5 on Pt(111) surfaces, investigated by means of HREELS and UPS. The adsorption of the molecules is different on the ordered and defect Nb_2O_5 surfaces.

Furthermore, the origin of acidic property of niobium oxide is discussed by these results, especially the structure and the oxygen vacancies.

2. Experimental

2.1. XAFS structure studies

2.1.1. Preparation of the samples for XAFS measurement

Highly acidic hydrated niobium oxide was prepared by following the literature [11]. The samples for XAFS measurement were hydrated niobium oxide, calcined at 393 K and 573 K in air stream and T-Nb_2O_5 (crystal), prepared by the heat-treatment of hydrated niobium oxide at 973 K in air. Furthermore, potassium salt of niobium isopolyacid, $K_8Nb_6O_{19}$, was prepared by fusing a mixture of T-Nb_2O_5 and KOH at around 873 K [12]. Formation of isopolyacid structure was confirmed by the X-ray diffraction method.

2.1.2. XAFS measurement

The Nb K-edge XAFS data were collected with an EXAFS apparatus (BL-10B) from the Photon Factory for High Energy Physics at Tsukuba. Photon energy was calibrated by the

measurement of niobium metal foil as a standard sample.

2.2. Preparation of thin films of niobium oxide on Pt(111) and adsorption of water, methanol and ethene on the NbO_x/Pt(111)

2.2.1. Preparation of thin films of niobium oxide on Pt(111)

The experiments described here were performed in a Leybold UHV chamber and the chamber is equipped to perform AES, UPS, ISS, EELS, LEED and mass spectrometry, as described elsewhere [13]. Previously, we reported the preparation of thin films of niobium oxide on Pt(111) single-crystal substrate [10]. The niobium oxide thin films were grown on the Pt(111) substrate by a stepwise process: (1) evaporation of about 0.1 monolayer (ML) niobium onto the Pt(111) substrate, (2) oxidation of the niobium with oxygen and (3) heating of the platinum substrate at 800–900 K to anneal and order the niobium oxide overlayer. And the oxygen vacancies of niobium oxide on Pt(111) were created by Ar^+ ion bombardment. The ion current used was 1×10^{-7} A at 500–1000 eV for 5 to 60 min. The structure of the niobium and niobium oxide was determined by means of LEED, HREELS and UPS. The atomic ratio of oxygen/niobium was estimated by ISS.

2.2.2. Adsorption of water, methanol and ethene on NbO_x/Pt(111)

Water adsorption was carried out by exposing water vapor to sample surfaces from back-filling the UHV chamber via a leak valve. Before being used for any exposure, the water was thoroughly degassed by freeze-thaw cycles. Methanol adsorption was carried out similarly. Ethene was introduced into the UHV chamber directly by back-filling with a leak valve. The vibration of adsorbed species was measured with HREELS with a primary energy of 4.0 eV and full width at half maximum in the elastic peak of typically 80–128 cm^{-1}.

3. Results and discussion

3.1. XAFS structure studies

Fig. 2 shows Nb K-edge adsorption spectra of hydrated niobium oxide, heat-treated at 393 K, T-Nb_2O_5 and $K_8Nb_6O_{19}$. The XAFS spectrum of hydrated niobium oxide, heat-treated at 573 K is similar to that of hydrated niobium oxide, heat-treated at 393 K. In the case of hydrated niobium oxide, the amplitude of vibration in the EXAFS region is small, compared with those for T-Nb_2O_5 and $K_8Nb_6O_{19}$. Fig. 3 shows the results of Fourier transformations of the EXAFS data for the niobium oxides. The distances and the coordination numbers of Nb–O and Nb–Nb bonds were determined by the curve-fitting analyses, as shown in Table 1. The corresponding peaks are indicated in Fig. 3. Although the dehydration of hydrated niobium oxide occurs by heat-treatment at 573 K [1], the distances and coordination numbers of Nb–O and Nb–Nb do not change substantially, thus, suggesting the retention of the skeleton of hydrated niobium oxide during the heat-treatment. This result is consistent with the fact that the acidity and catalytic activity of hydrated nio-

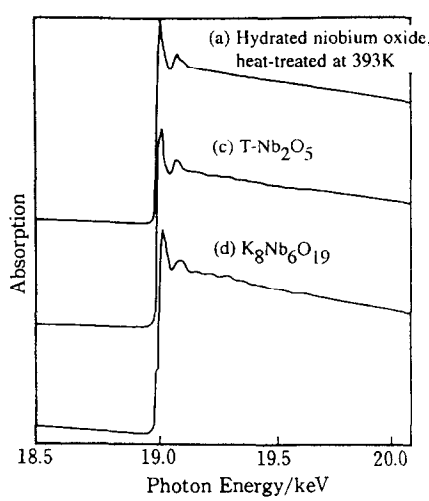

Fig. 2. Nb K-edge absorption spectra of (a) hydrated niobium oxide, heat-treated at 393 K, (c) T-Nb_2O_5 and (d) $K_8Nb_6O_{19}$. Measurement temperature: 70 K.

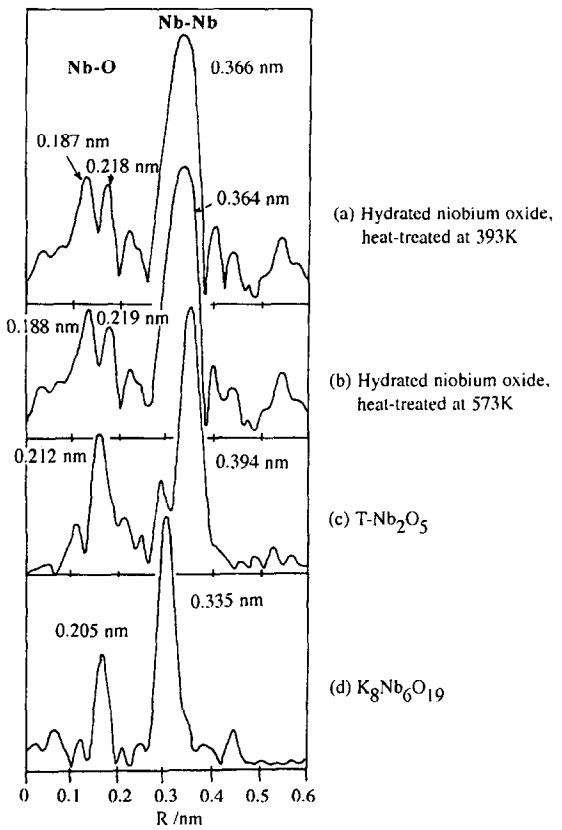

Fig. 3. Fourier transforms of Nb K-edge EXAFS data for (a) hydrated niobium oxide, heat-treated at 393 K, (b) hydrated niobium oxide, heat-treated at 573 K, (c) T-Nb_2O_5 and (d) $K_8Nb_6O_{19}$.

bium oxide, heat-treated at 573 K, are recovered again by exposing to H_2O vapor [1]. In other words, the dehydration and re-hydration of hydrated niobium oxide might occur without a structural change. The Nb–Nb distance of hydrated niobium oxide is intermediate between those of T-Nb_2O_5 and $K_8Nb_6O_{19}$. It might be due to the difference of the sharing of an O-atom in the NbO_6 octahedra among those oxides. Hence, the structure of hydrated niobium oxide seems to be different from that of the isopoly-acid, as shown in Fig. 1.

Furthermore, the Nb–O distances are significantly different from each other, among hydrated niobium oxide, T-Nb_2O_5 and $K_8Nb_6O_{19}$. There have been several papers for investigating the structure of niobium oxides [13]. There are several crystal modifications for Nb_2O_5, such as H-Nb_2O_5, P-Nb_2O_5, T-Nb_2O_5, N-Nb_2O_5, M-Nb_2O_5, R-Nb_2O_5. Some crystal structure of Nb_2O_5 has been characterized by means of X-ray diffraction and Raman spectroscopy. There are at least two types of Nb–O bonds existing for hydrated niobium oxide, as shown in Fig. 3. The short one is similar to the tetrahedral form of Nb–O and the longer one is similar to the octahedral form of Nb–O. The coordination number of tetrahedral form of Nb–O is larger than that of octahedral form of Nb–O. Tanabe et al. demonstrated the hypothesis for the generation of acid sites of binary metal oxides [14]. The hypothesis is as follows: (1) The coordination number of a positive element of a metal oxide, C_1 and that of a second metal oxide, C_2, are maintained even when mixed, (2) the coordination number of a negative element (oxygen) of a major component oxide is retained for all the oxygens in a binary oxide. In the case of hydrated niobium oxide, both of the positive elements are Nb, but the coordination numbers are different (tetrahedral and octahedral). The tetrahedral Nb–O seems to be superior to the octahedral Nb–O, because the coordination number of tetrahedral Nb–O is larger than that of octahedral Nb–O, as shown in Table 1. In this case, the excess of negative

Table 1
Curve fitting analyses of Fourier transforms of Nb K-edge EXAFS data for (a) hydrated niobium oxide, heat-treated at 393K, (b) hydrated niobium oxide, heat-treated at 573K, (c) T-Nb_2O_5 and (d) $K_8Nb_6O_{19}$

	Samples	Curve fitting analyses		
		Distance (R) (nm)	Coordination number (N; au)	R-factor (%)
Nb–O	(a) Hydrated	0.187	0.295	10.5
		0.218	0.116	8.7
	(b) Hydrated	0.188	0.287	11.4
		0.219	0.123	7.6
	(c) T	0.212	0.675	11.4
	(d)	0.205	0.889	9.4
Nb–Nb	(a)	0.366	0.381	2.0
	(b)	0.364	0.331	4.0
	(c)	0.394	1.12	7.0
	(d)	0.335	1.61	3.4

charge is present for Nb–O bond by applying Tanabe's hypothesis to single metal oxide consisting of at least two metal–O forms with different coordination number. Thus, the hydrated niobium oxide exhibits an acidity.

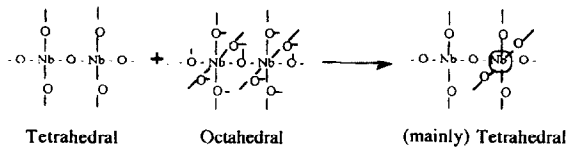

3.2. Preparation of thin films of niobium oxide on Pt(111) and adsorption of water, methanol and ethene on the NbO_x/Pt(111)

Preparation of thin films of niobium oxide on Pt(111) was described precisely elsewhere [10]. The thin films were made up of a high density of small crystallites on a epitaxial monolayer. The thin films of niobium oxide on Pt(111) was bombarded by 1000 eV Ar^+ ion for times from 5 to 30 min. ISS characterization shows that the oxygen-to-niobium ratio of the surface was decreased to about a third of the original value, as shown in Fig. 4. For bombardment times exceeding 5 min, LEED patterns were no longer seen. There were shifts in the AES and ILS signals that might indicate a decrease to lower oxidation states with bombardment. However, they were seen as small continuous shifts as a function of the bombardment times. It is diffi-

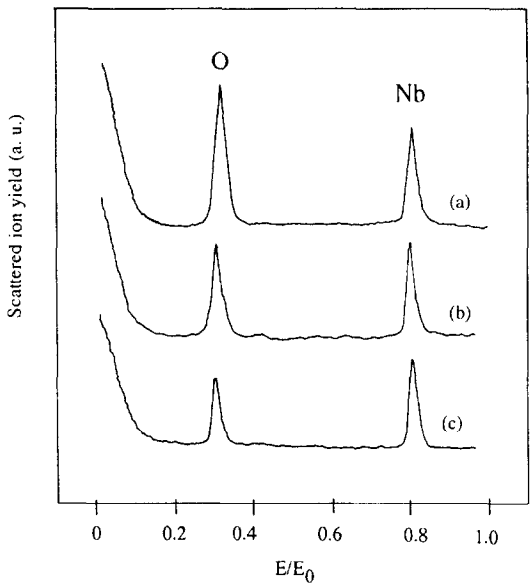

Fig. 4. ISS spectra of (a) an ordered Nb_2O_5 thin film, (b) a Nb_2O_5 thin film bombarded by 1000 eV Ar^+ ion for 10 min and (c) a Nb_2O_5 thin film bombarded by 1000 eV Ar^+ ion for 30 min.

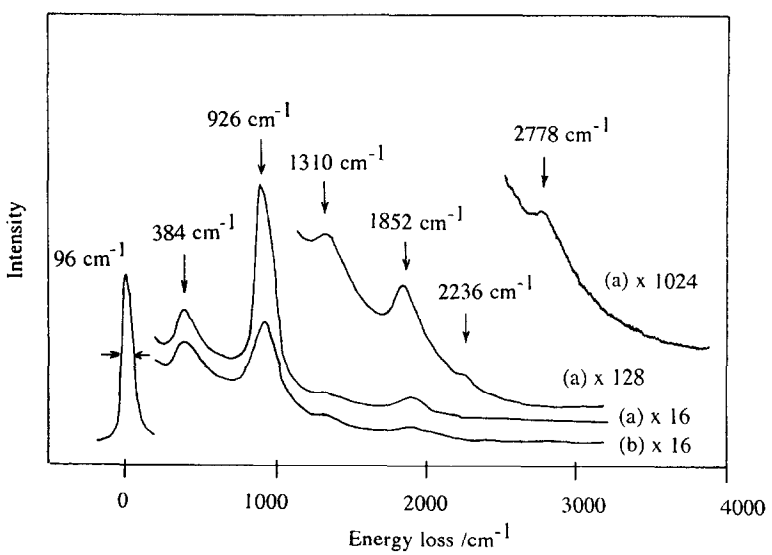

Fig. 5. HREELS of (a) a NbO_x thin film and (b) a Nb_2O_5 thin film on a Pt(111) substrate. The amounts of Nb deposited to make the thin films in (a) and (b) were equivalent to 3 layers.

cult to decide that these signals were actually made up of two signals from two different oxidation states whose composite signal gave a peak maximum appearing between the two peak maxima that should appear if they were resolved, because the resolution was not enough. Since, many of the energy shifts were seen at energies that were between the energies for NbO_x and Nb_2O_5, this latter interpretation might be true. This is consistent with the UPS data that showed the reduction of some Nb atoms to a lower oxidation state, while considerable amounts of Nb atoms remained in the 5 + state.

Figs. 5 and 6 show the HREELS of NbO_x thin film, Nb_2O_5 thin film and Ar^+ ion bombarded Nb_2O_5 thin film on Pt(111). The effects of Ar^+ ion bombardment are that the intensities of the photon vibrations decreased and there is a shift of the 926 cm^{-1} peak to 880 cm^{-1}. There is a possible asymmetry, perhaps due to a shoulder peak on the low-energy loss side, in the 880 cm^{-1} peak. In addition, a new loss feature appears at 536 cm^{-1}, after bombardment. The relative intensity of this peak increased with bombardment time.

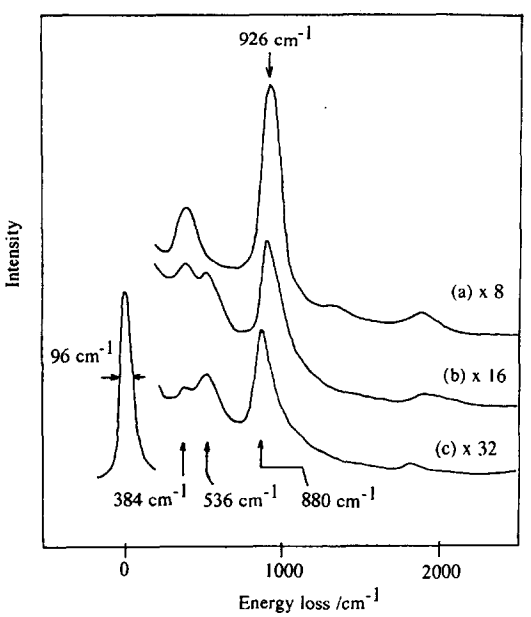

Fig. 6. HREELS of (a) the ordered Nb oxides surface, (b) the surface bombarded by 1000 eV Ar^+ ions for 10 min and (c) the surface bombarded by 1000 eV Ar^+ ions for 30 min.

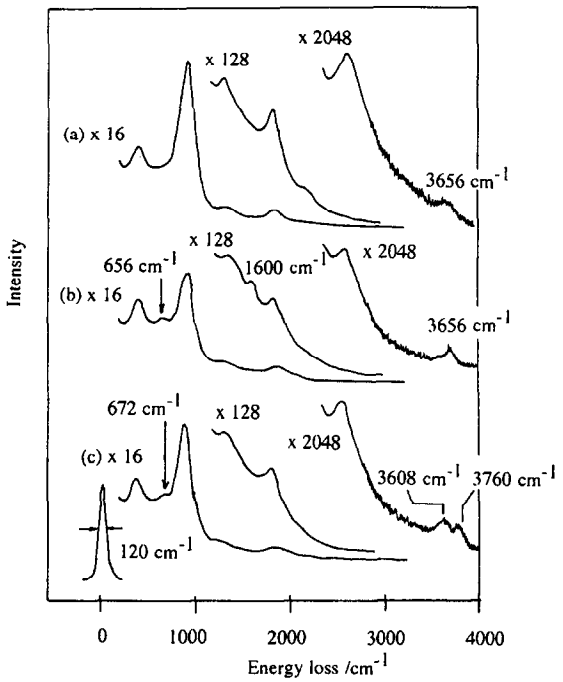

Fig. 7. HREELS of (a) a NbO_x thin film exposed to 30 L H_2O, (b) a Nb_2O_5 thin film exposed to 30 L H_2O and (c) an Ar^+ ion bombarded Nb_2O_5 thin film exposed to 30 L H_2O at room temperature.

Adsorption of water, methanol and ethene on the ordered NbO_x surface, the ordered Nb_2O_5 surface and the Ar^+ ion bombarded Nb_2O_5 surface were studied with UPS and HREELS.

Fig. 7 shows the HREEL spectra of water adsorbed to the three surfaces at room temperature. On the ordered Nb_2O_5 surface, three vibrational features are found at 656, 1600 and 3656 cm^{-1}. After exposure of the Ar^+ ion bombarded Nb_2O_5 surface, to water, three vibrational peaks at 672, 3608 and 3760 cm^{-1} are seen. The difference of UPS with exposures of water among the three Nb_2O_5 surface is not obvious.

When the Nb_2O_5 sample is heated, the vibrational features for water diminish but there is no qualitative change and the features disappear at 700 K. On the Ar^+ ion bombarded surface, the vibrational features decrease in intensity but are

still seen, even after heating of the sample for 30 min at 700 K. On the ordered NbO_x surface, the O–H stretch is seen at 3656 cm^{-1} after exposure at room temperature. This is still present after heating to 500 K and converts into two-peak spectrum with frequencies at 3608 and 3736 cm^{-1} on heating at 700 K, as shown in Fig. 8. This two-peak spectrum (curve c of Fig. 8) is qualitatively similar to the O–H stretch spectrum on the Ar^+ ion bombarded Nb_2O_5 surface.

The losses at 664, 1600 and 3656 cm^{-1} after exposing the Ar^+ ion bombarded Nb_2O_5 sample to 30 L water at room temperature are assigned to the excitations of ν(O–Nb) stretching modes, δ(HOH) scissor mode and the ν(OH) stretching modes. These agree with IR spectra and the losses of H_2O on Na_xWO_3, as shown in Table 2.

The HREEL spectrum of water adsorbed on

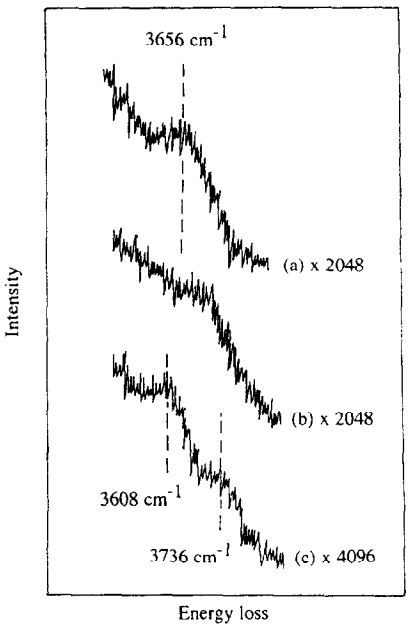

Fig. 8. HREELS of 30 L H_2O adsorbed on ordered NbO_x at (a) room temperature, (b) 500 K and (c) 700 K.

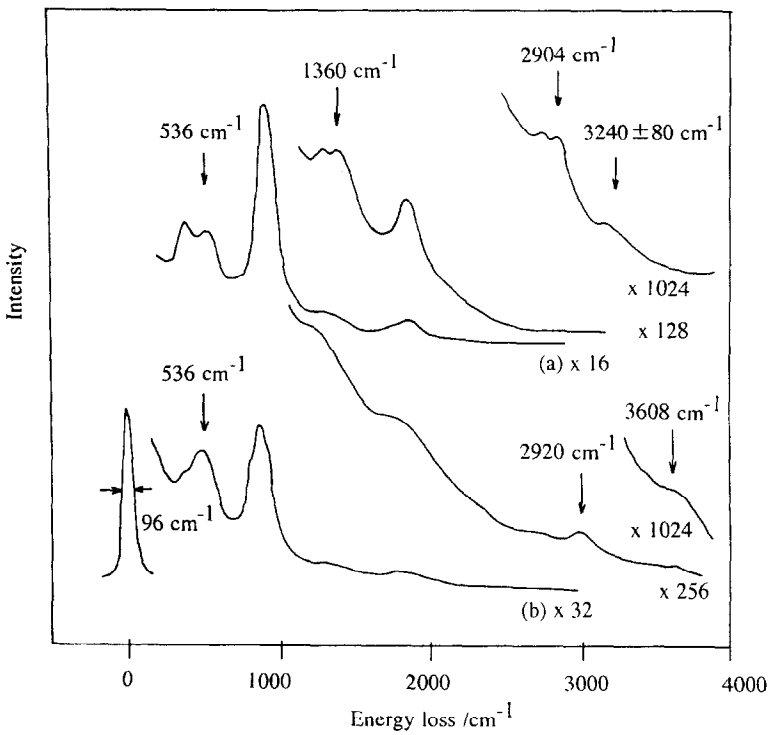

Fig. 9. HREELS of (a) an ordered Nb_2O_5 thin film exposed to 30 l CH_3OH and (b) an Ar^+ ion bombarded Nb_2O_5 thin film exposed to 30 L CH_3OH. (Temperature: adsorption of CH_3OH: 200 K, measurement of HREELS: room temperature).

Table 2
The vibrational frequencies and mode assignments for water vapor [15] and for molecular water on Na_xWO_3 single crystal [16]

	IR of H_2O vapor	H_2O on Na_xWO_3(100)	H_2O on the ordered Nb_2O_5
ν(O–M) (cm^{-1})	–	600	664
δ(HOH) (cm^{-1})	1595	1720	1600
ν(OH) cm^{-1}	3657 (s)	3560	3656
cm^{-1}	3757 (a)		

the Ar^+ ion bombarded (defect) Nb_2O_5 surface at room temperature is different from that on the ordered Nb_2O_5 surface. The loss at 664 cm^{-1} is still seen due to the excitation of the ν(O–Nb) stretching mode. The 3608 and 3760 cm^{-1} might be assigned to two kinds of surface hydroxyl ν(O–H) stretching modes. The vibration at 3760 cm^{-1} might be assigned to a hydroxyl formed on Nb cations. This assignment is supported by some reports on the observation that the formation of surface hydroxyls on metal and metal oxides results in an upward shift in the ν(OH) frequency [17] and the ν(OH) frequency on metal cations (here, called hydroxyl II) is higher than that on the surface O anions of metal oxides.

The peak at 3608 cm^{-1} might be assigned to hydroxyls with hydrogen atoms bonding to surface oxygen ions (here, called hydroxyl I). Its frequency could be predicted according to the formula [18]

$$[\omega(\text{O–H})_\text{I}]^2 = [\omega(\text{O–H})_\text{free}]^2 - [\omega(\text{Nb–O})_\text{I}]^2$$

where ω(O–H)$_\text{I}$ is the frequency of hydroxyl ν(OH) stretching mode, ω(O–H)$_\text{free}$ is the frequency of free O–H radicals and ω(Nb–O)$_\text{I}$ is the frequency of (Nb–O) stretching mode. Here, $\omega(\text{O–H})_\text{free} = 3664$ cm^{-1} [18], $\omega(\text{Nb–O})_\text{I} = 664$ cm^{-1}, then ω(O–H)$_\text{I}$ is 3603 cm^{-1} that is in good agreement with the experimental result of 3608 cm^{-1}.

Based on the results and assignments above, the conclusion can be made that water is dissociatively adsorbed on the defect Nb_2O_5 surface at room temperature and associatively adsorbed on the ordered NbO_x and Nb_2O_5 surface at room temperature, while water is dissociatively adsorbed on the ordered NbO_x surface on heating.

Fig. 9 shows the HREEL spectra of the ordered Nb_2O_5 thin film and the Ar^+ ion bombarded Nb_2O_5 thin film exposed to methanol. The adsorption of methanol to the Nb_2O_5 thin film was carried out at 200 K, while the HREELS was measured at room temperature. Direct exposure of methanol at room temperature results in the same HREEL spectra for the ordered Nb_2O_5 surface and for the defect Nb_2O_5 surface. Exposure of the samples to methanol gives rise to four distinct peaks at 536, 1360, 2904 and 3240 $\pm$ 80 cm^{-1}. The vibrational peak at 3240 $\pm$ 80 cm^{-1} disappears and a new peak at 3608 cm^{-1} takes its place on heating at 400 K, as shown in Fig. 10.

The vibration peaks of 536, 1360, 2904 and 3240 $\pm$ 80 cm^{-1} would be assigned to the Nb–O stretching mode due to the oxygen atoms of methanol bound to Nb cations of the Nb_2O_5

Table 3
The vibrational frequencies (cm^{-1}) and mode assignments for multilayer methanol on various single crystal metal and metal oxides and for gas-phase, liquid-phase and crystalline methanol

mode	Pt(111)	MgO(100)	gas-phase CH_3OH	liquid-phase CH_3OH	crystalline CH_3OH
ν(OH)	3220	3302	3681	3328	3328
ν a(CH)	2930	2947	2980	2980	2980
ν s(CH)			2840	2834	2834
δ(CH)	1410	1437	1455	1450	1480
ρ(CH)			1060	1135	1115
ν(CO)	970	1143	1033	1030	1030
π(CH)	680			655	655
Ref.	[18]	[19]	[20]	[20]	[21]

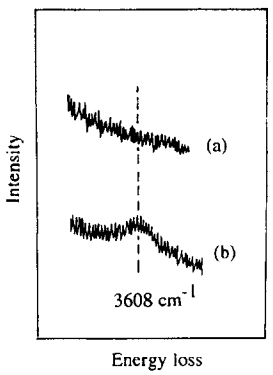

Fig. 10. HREELS of adsorbed CH_3OH on ordered Nb_2O_5 at (a) room temperature and (b) 400 K.

surface, CH_3 bending mode ($\delta(CH_3)$), C–H stretching mode ($\nu(CH)$) and O–H stretching mode ($\nu(OH)$), respectively. This assignments are supported by the reports of the observation of CH_3OH adsorbed on other metal and metal oxides, as shown in Table 3.

On the ordered Nb_2O_5 surface, methanol seems to be adsorbed molecularly at room temperature. Annealing of the sample to 400 K resulted in disappearance of the 3240 cm^{-1} loss and the appearance of a new peak at 3608 cm^{-1}, which is identical to the vibration assigned to hydroxyl I species from water adsorption, indicates the dissociation of methanol and the formation of a methoxy species upon heating. Exposing the defect Nb_2O_5 surface to methanol at room temperature gave rise to several losses at 536, 2920 and 3608 cm^{-1}, which are similar to the losses of methanol from the ordered Nb_2O_5 surface heated to 400 K.

On the ordered NbO_x and Nb_2O_5 surface, no evidence of ethene adsorption at 200 K is found by HREELS. On the other hand, exposing 100 L ethene to the defect Nb_2O_5 surface at about 200 K in HREELS gives a weak vibration peak at 1500 cm^{-1}, as shown in Fig. 11. Information about ethene adsorption available from HREELS is limited due to the very strong surface optical photons on niobium oxides which overlapped the weaker vibration of ethene adsorption. However, there are at least four vibration peaks appeared after exposure of ethene to the defect Nb_2O_5 surface. The vibration peaks at 920, 1800 and 1500 cm^{-1} can be assigned to the C–H out-of-plane wag mode and its overtone vibration and the $\nu(C{=}C)$ stretching mode. It implies that ethene is adsorbed molecularly on the defect Nb_2O_5 surface with a π-complex formation. There are no obvious features found in the HREELS after exposure of the ordered NbO_x and Nb_2O_5 surface to ethene. This means the coverage of ethene on the ordered niobium oxides surface is less than the limit of detectability.

There are different behaviors of adsorption of water, methanol and ethene between on the

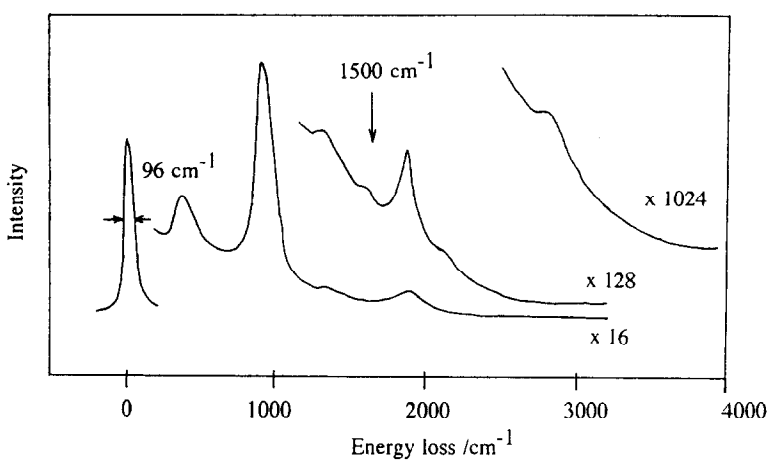

Fig. 11. HREELS of an Ar^+ ion bombarded Nb_2O_5 thin film exposed to 100 L C_2H_4.

ordered niobium oxides surface and on the defect Nb_2O_5 surface. The defects from the formation of oxygen vacancies seem to play an important role in the adsorption of molecules on oxides surface. Water and methanol are adsorbed associatively on the ordered niobium oxide surface at room temperature and the adsorption of ethene is weak. But on the defect Nb_2O_5 surface, dissociative adsorption of water and methanol takes place and the adsorption of ethene is stronger. The oxygen vacancies seem to be related to the origin of the acidity of niobium oxide.

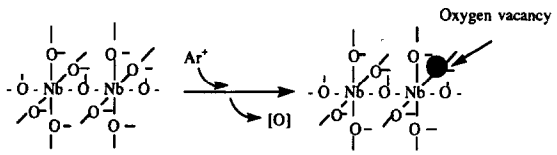

4. Conclusions

The structure of niobium oxides was investigated by using XAFS and surface science technique. The origin of acidic property and catalysis of niobium oxide are discussed by these results.

The following key points emerge from this study:

(1) The structure of highly acidic hydrated niobium oxide was studied by XAFS, compared with those of T-Nb_2O_5 (crystal) and niobium isopolyacid potassium salt ($K_8Nb_6O_{19}$), which had been previously demonstrated as the structure of hydrated niobium oxide. The curve-fitting analyses show that Nb–Nb distances are different among the niobium oxides, namely, $K_8Nb_6O_{19}$ (0.335 nm) < hydrated niobium oxide (0.365 nm) < T-Nb_2O_5 (0.394 nm). Furthermore, the Nb–O distances are significantly different from each other. Hence, the structure of hydrated niobium oxide is different from those of T-Nb_2O_5 and $K_8Nb_6O_{19}$.

(2) There are at least two types of Nb–O bonds existing for hydrated niobium oxide. The short one is similar to the tetrahedral form of Nb–O and the longer one is similar to the octahedral form of Nb–O. The coordination number of tetrahedral form is larger than that of octahedral form. The excess of negative charge is present for Nb–O bond by applying Tanabe's hypothesis to single metal oxide consisting of at least two metal–O forms with different coordination number. Thus, the hydrated niobium oxide exhibits an acidity.

(3) Although the dehydration of hydrated niobium oxide occurs by heat-treatment at 573 K, the distances and coordination numbers of Nb–O and Nb–Nb do not change substantially, thus, suggesting the retention of the skeleton of hydrated niobium oxide during the heat-treatment.

(4) The preparation and adsorption of ordered niobium oxides thin film on Pt(111) and their defect face were studied by using UHV surface analysis apparatus comprising AES, LEED, UPS, ISS and HREELS. The oxygen vacancies of niobium oxide on Pt(111) were created by Ar^+ ion bombardment.

(5) H_2O and CH_3OH exhibit associated adsorption on the ordered NbO_x and Nb_2O_5 surface and dissociative adsorption on the defect Nb_2O_5 surface at room temperature. At higher temperature, H_2O and CH_3OH are adsorbed dissociatively on the ordered NbO_x surface. These results imply that oxygen vacancies of NbO_x surface play an important role on the adsorption of molecules.

(6) On the ordered NbO_x and Nb_2O_5 surface, no evidence of ethene adsorption at 200 K is found by HREELS, although ethene is adsorbed molecularly on the defect Nb_2O_5 surface with a π-complex formation.

References

[1] T. Iizuka, K. Ogasawara and K. Tanabe, Bull. Chem. Soc. Jpn., 56 (1983) 2927.
[2] Z. Chen, T. Iizuka and K. Tanabe, Chem. Lett. (1984) 1085.
[3] T. Iizuka, S. Fujie, T. Ushikubo, Z. Chen and K. Tanabe, Appl. Catal., 28 (1986) 1.

[4] T. Ushikubo, Y. Hara and K. Wada, Catal. Today, 16 (1993) 525.
[5] G. Neumann, Acta. Chem. Scand., 18 (1964) 278.
[6] B.K. Sen, A.V. Saha and N. Chatterjee, Mat. Res. Bull., 16 (1981) 923; B.K. Sen and A.V. Saha, Mat. Res. Bull., 17 (1982) 161; B.K. Sen, P. Bandyopadhyay and A.V. Saha, Mat. Res. Bull., 17 (1982) 611.
[7] V. Bardi, P.N. Ross and G.A. Somorjai, J. Vac. Sci. Technol., A2 (1984) 40.
[8] G.H. Vurens, M. Salmeron and G.A. Somorjai, Surf. Sci., 201 (1988) 129.
[9] K.B. Lewis, S.T. Oyama and G.A. Somorjai, Surf. Sci., 233 (1990) 74.
[10] L. Xie, D. Wang, C. Zhong, X. Guo, T, Ushikubo and K. Wada, Surf. Sci., 320 (1994) 62.
[11] T. Ushikubo, T. Iizuka, H. Hattori and K. Tanabe, Catal. Today 16 (1993) 291.
[12] G.M. Walterman, Jpn. Patent Application 59207806.
[13] B.M. Gatehouse and A.D. Wadsley, Acta Cryst., 17 (1964) 1545; S. Andersson, Z. Anorg. Allg. Chem., 3351 (1967) 106; A.A. McConell, J.S. Anderson and C.N.R. Rao, Spectrochimica Acta, 32A (1976) 1067; U. Balachandran and N.G. Eror, J. Mat. Sci. Lett., (1982) 374; B. Meyer and R. Gruehn, Z. Anorg. Allg. Chem., 484 (1983) 77; G. Heurung and R. Gruehn, Z. Anorg. Allg. Chem., 491 (1982) 101; G. Brauer, Z. Anorg. Allg. Chem., B248 (1941) 1.
[14] K. Tanabe, T. Sumiyoshi, K. Shibata, T. Kiyoura and J. Kitagawa, Bull. Chem. Soc. Jpn., 47 (1974) 1064.
[15] H. Ibach and D.L. Mills, Electron energy loss spectroscopy and surface vibrations, Academic Press, New York, 1982, p. 348.
[16] R.G. Egdell, Adsorption and catalysis on oxide surface, Elsevier, Amsterdam, 1985, 173.
[17] P.A. Thiel and T.E. Madey, Surf. Sci. Rep., 7 (1987) 211; S. Andersson and J.W. Daveport, Solid State Commun., 28 (1978) 677; J.G. Chen, T.E. Crowell and J.T. Yates, J. Chem. Phys., 84 (1986) 5904.
[18] B.A. Sexlon, Surf. Sci., 102 (1981) 271.
[19] M.C. Wu and D.W. Goodman, Catal. Lett., 15 (1992) 1.
[20] A. Falk and E. Whalley, J. Chem. Phys., 34 (1961) 1554.
[21] A.B. Dempster and G. Zerbi, J. Chem. Phys., 54 (1971) 3600.